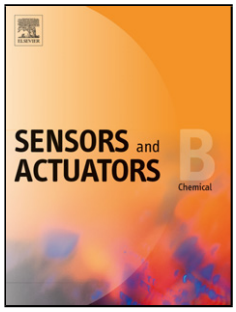


Title: Increased Volume Responsiveness of Macroporous Hydrogels

Authors: Andrew E. Coukouma, Sanford A. Asher

PII: S0925-4005(17)31775-6
DOI: http://dx.doi.org/10.1016/j.snb.2017.09.109
Reference: SNB 23200

To appear in: *Sensors and Actuators B*

Received date: 8-8-2017
Accepted date: 17-9-2017

Please cite this article as: Andrew E.Coukouma, Sanford A.Asher, Increased Volume Responsiveness of Macroporous Hydrogels, Sensors and Actuators B: Chemicalhttp://dx.doi.org/10.1016/j.snb.2017.09.109

# Increased Volume Responsiveness of Macroporous Hydrogels

Andrew E. Coukouma and Sanford A. Asher

Department of Chemistry, University of Pittsburgh, Pittsburgh, Pennsylvania 15260, USA

asher@pitt.edu

Fax: +1 412 624 0588; Tel: +1 412 624 8570

## Highlights

- Determined that the magnitude of the hydrogel VPT increases with increasing void volumes
- Hydrogel VPT increased by 3 to10-fold due to the incorporation of voids
- The incorporation of voids decreases the elastic free energy induced osmotic pressure
- Macroporous hydrogels appear more mechanically robust than non-macroporous hydrogels

## Abstract

Hydrogels can be fabricated into smart materials whose volumes predictably depend on their chemical environment. These smart hydrogel materials can be utilized in applications such as sensors, actuators, and for drug delivery materials, for example. The volume response of these hydrogels is well-known to be limited by their crosslink density. Thus, the responsiveness of hydrogels can be increased by decreasing the hydrogel's crosslink density. Unfortunately, this also decreases the hydrogel strength.

The hydrogel "effective crosslink density" can be decreased by fabricating macroporous hydrogels where voids are incorporated into the hydrogel. In the work here we demonstrate that this approach increases the volume responsiveness of hydrogels. We fabricated pH responsive macroporous hydrogels by copolymerizing acrylic acid with acrylamide. We compared the pH response of these hydrogels to that of macroporous hydrogels with small water bubbles embedded by vortexing the polymerizing hydrogel in air, or by preparing an inverse opal hydrogel. We then filled these embedded air bubbles with water. The pH responsiveness of these macroporous hydrogels are significantly increased compared to those of non-macroporous hydrogels of similar composition. We find that these macroporous hydrogels appear to be more mechanically robust than are similarly responsive hydrogels without voids.

## Highlights

- Determined that the magnitude of the hydrogel VPT increases with increasing void volumes
- Hydrogel VPT increased by 3 to10-fold due to the incorporation of voids
- The incorporation of voids decreases the elastic free energy induced osmotic pressure
- Macroporous hydrogels appear more mechanically robust than non-macroporous hydrogels

**Keywords:** Hydrogels; Volume Phase Transitions; Macroporous Hydrogels; Inverse Opals; Hydrogel Sensors

## 1. Introduction

Hydrogels are crosslinked polymer materials that contain significant amounts of a water mobile phase. Hydrogels can be fabricated into highly responsive "smart" materials that respond to changes in their chemical or physical environments. Hydrogels imbibe or expel water in response to changes in their chemical environment, by undergoing a Volume Phase Transition (VPT)[1]. Hydrogels have been utilized in sensors [2-8], actuators [9, 10], and other smart material applications [11-13]. There is great interest in developing hydrogel sensors to sensitively and selectively detect changes in their chemical and physical environments such as pH [14-17] and heavy metal concentrations [7, 18, 19], temperature [20-22], and, most recently, concentrations of microbes [4].

Flory demonstrated that hydrogel VPT result from osmotic pressures derived from the free energy of mixing, from counter ion concentration inhomogeneitiy free energies, and from the crosslinking elastic free energy [1]. The magnitude of the hydrogel VPT is constrained by the hydrogel crosslink density. Obviously, we can increase the magnitude of the VPT by decreasing the hydrogel crosslink density. However, this will decrease the mechanical strength of the resulting hydrogel [3]. In the work here we attempt to decrease the "effective crosslinking density" by introducing voids into the hydrogels.

We formed two types of macroporous hydrogels by either incorporating lots of small air and water bubbles into a polymerizing hydrogel by vortexing the system, or by forming an inverse opal hydrogel [16, 19, 23, 24]. Inverse opal hydrogels are fabricated by polymerizing a hydrogel polymer monomer solution around close packed monodisperse particles. Similar inverse opal hydrogels have been utilized in sensing [16, 19, 24] and cell growth [23, 25] applications.

## 2. Materials and Methods

*2.1 Materials*

Igracure 2959, Acrylamide (Am), Azobisisobutyronitrile (AIBN), Pluronic F-127 (PF-127), Sodium Phosphate Monobasic, Sodium Phosphate Dibasic, Ammonium Persulfate (AMPS), N,N,N',N'-Tetramethylethane-1,2-diamine (TEMED) , Tetrahydrofuran (THF) and N-N`-Methylenebisacrylamide (BIS) were acquired from Sigma Aldrich (≥95% purity) and used as received. Acrylic acid (AA) was acquired from Sigma Aldrich and purified through distillation. Glacial acetic acid and ethylene glycol was supplied by Fisher and used as received. Sodium acetate was acquired from EM Science and used as received. Water was purified by a Barnstead nanopure system.

*2.2 Fabrication of inverse opal hydrogels*

Fig. 1 shows the fabrication of inverse opal macroporous hydrogels. A close packed array of monodisperse 940 nm polystyrene particles was formed by evaporating 2 mL of a ~15% (w/w) dispersion of these particles on a glass slide (Figure 1A). Igracure 2495 was used to initiate the polymerization of 150 μL of a solution of 10% (w/w) AAm, 1% (w/w) AA, and 1% (w/w) BIS in a 50% ethylene glycol -50%water solution. This polymerization solution was layered onto the previously prepared dried close packed polystyrene particles (Figure1B). A glass slide was placed on top of the solution for 30 min to allow the polymerization solution to fill the polystyrene particles interstitial spaces. The system was then exposed to UV light from two Blak Ray 365 nm mercury lamps for 15 min to polymerize the opal hydrogel (Figure1C). The opal hydrogel was then peeled from the glass slides and soaked in THF for 12 hrs. to

dissolve the polystyrene particles (Figure1C to D). The resulting inverse opal hydrogel was stored in pH ~3 sodium acetate buffer.

*2.3 Fabrication of vortexed hydrogels*

Vortexed hydrogels were prepared by deoxygenating 6 mL of a 10% (w/w) AAm, 1%(w/w) AA, 1% (w/w) BIS in a 50% ethylene glycol - 50% water solution by bubbling with $N_2$ gas for 30 min (Figure 1E). 400 μL of a 20% (w/w) solution of PF-127 in water was injected into this deoxygenated solution and gently mixed. To initiate polymerization 100 μL each of 10% (w/w) TEMED in water, and 10% (w/w) AMPS in water were injected into the vial (Figure 1F). The monomer solution was then agitated by vortexing to incorporate gas bubbles during the polymerization (Figure 1 G to H). After polymerization (~ 3-5 min), the macroporous hydrogel was removed from the vial and stored in pH ~3 sodium acetate buffer. Non-macroporous samples were similarly fabricated, but without vortexing.

*2.5 Electron microscopy of hydrogels.*

The hydrogels were characterized by Scanning Electron Microscopy (JEOL JSM-6390LV). Samples were dried in air at room temperature and were then sputter coated with a thin layer of Au.

*2.4 Measurement of pH volume response*

The pH volume responses of the macroporous hydrogels were monitored by swelling ratio measurements. Hydrogel samples were prepared for swelling ratio measurements by washing with water over 24 hrs. to remove residual ethylene glycol and THF. The hydrogel samples were then dried in air at 75°C for 24 hrs, after which their dry weight was measured.

The samples were then placed in sodium acetate buffers (pH 3.5-6) or sodium phosphate buffers pH (6-7.5) for 24 hrs (Figure 1 I). The ionic strength of the buffers was maintained at 0.01 M to avoid volume alterations due to changes in ionic strength. The hydrogels in buffer were subjected to vacuum for 30-60 sec. to assure that all voids were filled with buffer.

The wet, swollen, hydrogel weights were measured by removing the samples from the buffer and gently patting their exterior with an absorbent kimwipe before weighing the samples. This process was replicated several times and the results averaged. The swelling ratio, Q is defined as $\boldsymbol{Q = (Weight\ Wet - Weight\ Dry)/Weight\ Dry}$ **(1)**

## 3. Results and Discussion

*3.1 Structure and morphology of vortexed hydrogels.* The morphology of the macroporous hydrogels fabricated by vortexing were compared to those of non-macroporous hydrogels by SEM (Figure 2). The SEM image of the vortexed macroporous hydrogel shows the presence of numerous large pores between 10-100 μm in diameter, (Figure 2A). This contrasts to the non-macroporous hydrogels that do not show pores (Figure 2B). The inverse opal hydrogels did not show clear SEM images, presumably because of their low polymer hydrogel volume fractions which caused them to collapse on drying.

*3.2 pH volume phase transitions of macroporous hydrogels*

We fabricated pH responsive hydrogels by copolymerizing acrylic acid which has a pKa of ~4.7[14]. At elevated pH values the hydrogel carboxyl groups deprotonate attaching charges to the hydrogel network. These charges localize counterions around them that generate osmotic pressures that swell the hydrogel.

According to Flory-Huggins theory, the osmotic pressure induced by the deprotonation of the carboxyl group is counterbalanced by the osmotic pressure from the crosslinked hydrogel network [1]. The crosslinked hydrogel network osmotic pressure is dominated by the polymer chain crosslinks. However, the introduction of voids in the hydrogel network affects the hydrogel elasticity and its mechanical properties [26]. The voids decrease the contribution of the elastic free energy to the osmotic pressure due the decrease in the hydrogel polymer network volume fraction. This decrease in the elastic free energy contributions should increase the magnitude of the hydrogel VPT.

Thus, macroporous hydrogels are expected to have an increased VPT pH response compared to that of non-macroporous hydrogels. To confirm this expectation, we compared the pH dependence of the swelling ratio, Q of macroporous to non-macroporous, hydrogels (Figure 3), where Q, was calculated as shown in Eq 1.

Between pH 3.2 to 4.1 the non-macroporous hydrogel responsivity, ($\Delta Q/\Delta pH$) is 0.92±0.08. A ~3-fold larger responsivity occurs for the macroporous vortexed hydrogel (2.6±0.2). The responsivity is increased 10-fold compared to the, non-macroporous hydrogel for the inverse opal hydrogel (9.9±0.4). A vortexed hydrogel in the absence of acrylic acid shows no significant volume response over this same pH range.

We examined the dependence of hydrogel pH responsivity on the effective relative crosslinker concentration (Figure 4). We expect that effective relative crosslinker concentration will scale as the product of the crosslinker concentration ($C_C$) added, and polymer volume fraction, as decreased by the incorporated voids: ERC=$C_c$ $(1 - f)$, where f is the void volume fraction; the hydrogel volume fraction = 1 for the non-macroporous hydrogels.

The macroporous hydrogel volume fraction was determined from the measured hydrogel density. The hydrogel densities were determined from the weights and volumes of the hydrogel samples. The hydrogel density is the volume fraction weighted sum of the water equilibrated hydrogel density and the water filled void density, assumed to be that of water,

$\rho_{MH} = \rho_w f + \rho_H (1-f)$, where $\rho_{MH}$ is the macroporous hydrogel density, $\rho_w$ is the density of the hydrogel water bubbles and $\rho_H$ is the density of the non-macroporous pure hydrogel.

We prepared both a vortexed and an inverse opal macroporous hydrogel. From their measured densities we calculated that the vortexed hydrogel volume fraction, to be 0.55, while the inverse opal hydrogel volume fraction was 0.30. A perfect close packed inverse opal hydrogel would have volume fraction of 0.26. Our hydrogel volume fractions were generally larger, due to a lack of close packing. The hydrogel pH responsivity, as shown in Figure 4, is inversely proportional to the ERC. This is expected due to the expected non-linear inverse relationship between the number of crosslinks and the hydrogel swelling ratio [1, 6]

We prepared hydrogels with different ERC by varying the BIS crosslinker concentrations between 0.5 and 1 % for vortexed and inverse opal hydrogels. We found that we could prepare an *inverse opal hydrogel* with an estimated ERC ~0.3 % that shows a responsivity of ~14.3 by using a 1% BIS crosslinker concentration and a hydrogel volume fraction of 0.3. Alternatively, we prepared a vortexed hydrogel with the same responsivity of ~14.3 by using 0.5% BIS and a hydrogel volume fraction of 0.55. Interestingly, the vortexed hydrogel with 0.5% BIS appears to have significantly lower mechanical strengths; the hydrogel broke into multiple pieces after 3 swelling ratio measurements. In contrast, the inverse opal hydrogel with 1 % BIS appears more mechanically robust; it did not fall apart after 3 measurement cycles.

This increased mechanical robustness presumably results from a decreased hydrogel brittleness due to the increase numbers of hydrogel voids which decreases the ability of fractures to successfully propagate [27, 28]. For example, voids in foam-like structures interfere with fracture propagation in metallic foams [29]. Thus, we conclude that increasing the void volumes in hydrogels should decrease fracture propagation, which should increase their mechanical strength.

## 4. Conclusion

We demonstrated an increased magnitude of VPT of macroporous hydrogels compared to those of non-macroporous hydrogels. We conclude that the incorporation of voids into the hydrogel network decreases the impact of the hydrogel crosslinking network elastic free energy constraints, which enables an increased hydrogel response. An increased magnitude of the VPT enables the fabrication of more responsive chemical sensors which enable lower limits of detection. We also demonstrated novel and simple vortexing and inverse opal fabrication methods that enable easy fabrication of macroporous hydrogels. These macroporous hydrogels appear more mechanically robust than their non-macroporous counterparts.

## Acknowledgements

We thank Dr. Sachin Velankar for discussions about the mechanical properties of hydrogel materials. We would like to acknowledge the Defense Threat Reduction Agency (DTRA) for supporting this work (Grant No. HDTRA 1-15-1-0038)

## References

[1] P.J. Flory, Principles of polymer chemistry: Cornell University Press; 1953.

[2] Z. Cai, L.A. Luck, D. Punihaole, J.D. Madura, S.A. Asher, Photonic crystal protein hydrogel sensor materials enabled by conformationally induced volume phase transition, Chemical Science, 7(2016) 4557-62.
[3] A.E. Coukouma, N.L. Smith, S.A. Asher, Removable interpenetrating network enables highly-responsive 2-D photonic crystal hydrogel sensors, Analyst, 140(2015) 6517-21.
[4] Z. Cai, D.H. Kwak, D. Punihaole, Z. Hong, S.S. Velankar, X. Liu, et al., A Photonic Crystal Protein Hydrogel Sensor for Candida albicans, Angewandte Chemie International Edition, 54(2015) 13036-40.
[5] J.-T. Zhang, L. Wang, J. Luo, A. Tikhonov, N. Kornienko, S.A. Asher, 2-D Array Photonic Crystal Sensing Motif, Journal of the American Chemical Society, 133(2011) 9152-5.
[6] A.V. Goponenko, S.A. Asher, Modeling of Stimulated Hydrogel Volume Changes in Photonic Crystal Pb2+ Sensing Materials, Journal of the American Chemical Society, 127(2005) 10753-9.
[7] S.A. Asher, A.C. Sharma, A.V. Goponenko, M.M. Ward, Photonic crystal aqueous metal cation sensing materials, Analytical chemistry, 75(2003) 1676-83.
[8] J.H. Holtz, S.A. Asher, Polymerized colloidal crystal hydrogel films as intelligent chemical sensing materials, Nature, 389(1997) 829-32.
[9] G. Gerlach, K.-F. Arndt, Hydrogel sensors and actuators: engineering and technology: Springer Science & Business Media; 2009.
[10] Z. Liu, P. Calvert, Multilayer hydrogels as muscle- like actuators, Advanced Materials, 12(2000) 288-91.
[11] A.S. Hoffman, Hydrogels for biomedical applications, Advanced drug delivery reviews, 64(2012) 18-23.
[12] Y. Qiu, K. Park, Environment-sensitive hydrogels for drug delivery, Advanced drug delivery reviews, 64(2012) 49-60.
[13] B. Jeong, S.W. Kim, Y.H. Bae, Thermosensitive sol–gel reversible hydrogels, Advanced drug delivery reviews, 54(2002) 37-51.
[14] A. Richter, G. Paschew, S. Klatt, J. Lienig, K.-F. Arndt, H.-J.P. Adler, Review on hydrogel-based pH sensors and microsensors, Sensors, 8(2008) 561-81.
[15] J.E. Elliott, M. Macdonald, J. Nie, C.N. Bowman, Structure and swelling of poly (acrylic acid) hydrogels: effect of pH, ionic strength, and dilution on the crosslinked polymer structure, Polymer, 45(2004) 1503-10.
[16] Y.J. Lee, P.V. Braun, Tunable inverse opal hydrogel pH sensors, Advanced Materials, 15(2003) 563-6.
[17] S.H. Gehrke, E.L. Cussler, Mass transfer in pH-sensitive hydrogels, Chemical Engineering Science, 44(1989) 559-66.
[18] S.A. Asher, S.F. Peteu, C.E. Reese, M. Lin, D. Finegold, Polymerized crystalline colloidal array chemical-sensing materials for detection of lead in body fluids, Analytical and bioanalytical chemistry, 373(2002) 632-8.
[19] M.-L. Zhang, F. Jin, M.-L. Zheng, X.-M. Duan, Inverse opal hydrogel sensor for the detection of pH and mercury ions, RSC Advances, 4(2014) 20567-72.
[20] M.J. Snowden, B.Z. Chowdhry, B. Vincent, G.E. Morris, Colloidal copolymer microgels of N-isopropylacrylamide and acrylic acid: pH, ionic strength and temperature effects, J Chem Soc, Faraday Trans, 92(1996) 5013-6.
[21] H. Kanazawa, K. Yamamoto, Y. Matsushima, N. Takai, A. Kikuchi, Y. Sakurai, et al., Temperature-responsive chromatography using poly (N-isopropylacrylamide)-modified silica, Analytical chemistry, 68(1996) 100-5.
[22] K. Otake, H. Inomata, M. Konno, S. Saito, Thermal analysis of the volume phase transition with N-isopropylacrylamide gels, Macromolecules, 23(1990) 283-9.
[23] A.N. Stachowiak, D.J. Irvine, Inverse opal hydrogel- collagen composite scaffolds as a supportive microenvironment for immune cell migration, Journal of Biomedical Materials Research Part A, 85(2008) 815-28.

[24] Y.-J. Lee, S.A. Pruzinsky, P.V. Braun, Glucose-sensitive inverse opal hydrogels: analysis of optical diffraction response, Langmuir, 20(2004) 3096-106.
[25] M.C. Ford, J.P. Bertram, S.R. Hynes, M. Michaud, Q. Li, M. Young, et al., A macroporous hydrogel for the coculture of neural progenitor and endothelial cells to form functional vascular networks invivo, Proceedings of the National Academy of Sciences of the United States of America, 103(2006) 2512-7.
[26] T. Nakajima, H. Furukawa, Y. Tanaka, T. Kurokawa, J.P. Gong, Effect of void structure on the toughness of double network hydrogels, Journal of Polymer Science Part B: Polymer Physics, 49(2011) 1246-54.
[27] L. Weng, A. Gouldstone, Y. Wu, W. Chen, Mechanically strong double network photocrosslinked hydrogels from N, N-dimethylacrylamide and glycidyl methacrylated hyaluronan, Biomaterials, 29(2008) 2153-63.
[28] J.-Y. Sun, X. Zhao, W.R. Illeperuma, O. Chaudhuri, K.H. Oh, D.J. Mooney, et al., Highly stretchable and tough hydrogels, Nature, 489(2012) 133.
[29] Y. Sugimura, J. Meyer, M. He, H. Bart-Smith, J. Grenstedt, A. Evans, On the mechanical performance of closed cell Al alloy foams, Acta Mater, 45(1997) 5245-59.

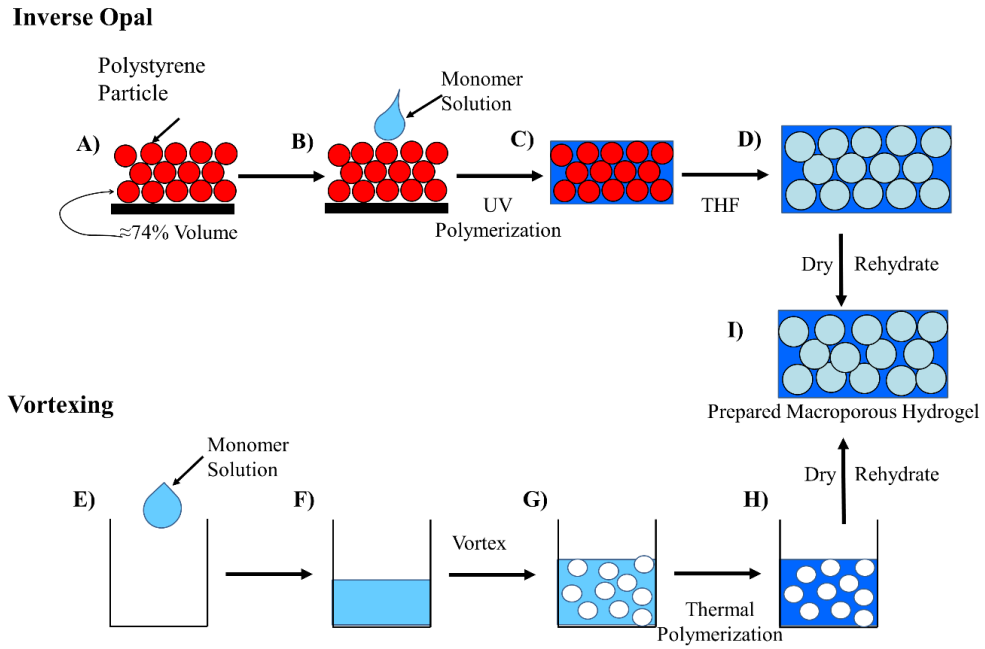


**Figure 1 Fabrication methods utilized to produce macroporous hydrogels. A-D. An inverse opal method utilizes polstrene nanoparticles to incorporate macropores. E-H. Alternatively, a vortexing method utilizes agitation to incorporate air bubble macropores. Macroporous hydrogels fabricated via both methods were dried and rehydrated, filling the air bubbles with water before the swelling ratio measurements.**

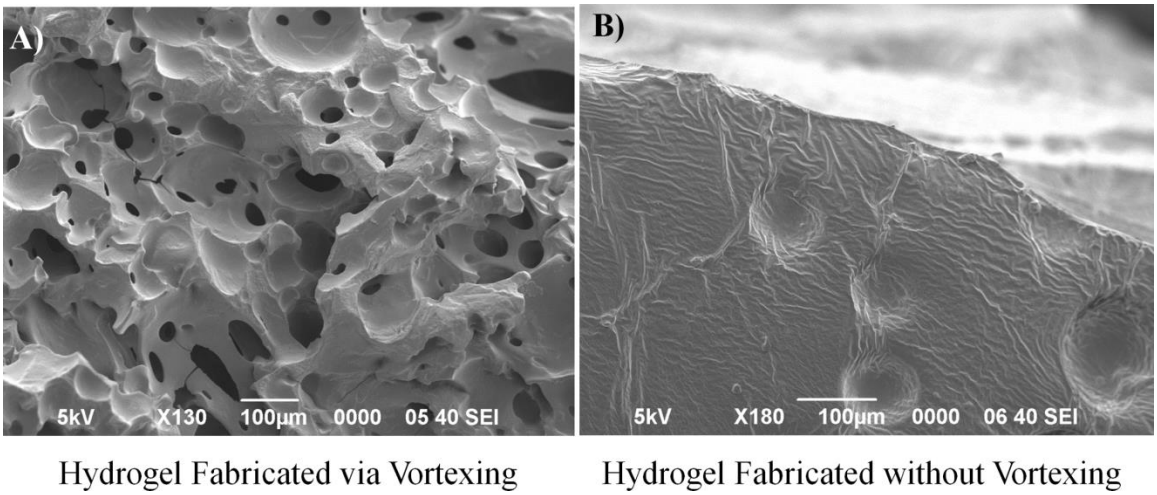


**Figure 2 SEM micrographs. A. Hydrogel fabricated using the vortexing method shows large pores of 10-100 µm in diameter. B. A non-macroporous hydrogel shows no pores**

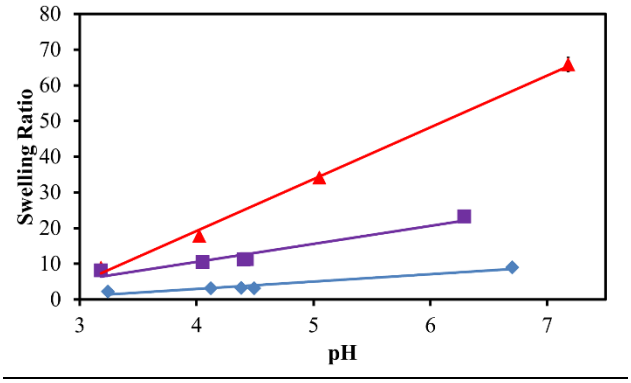


**Figure 3 Comparison of pH dependence of the swelling ratio of macroporous hydrogels compared to a non-macroporous hydrogel. Error bars indicate one standard deviation.**

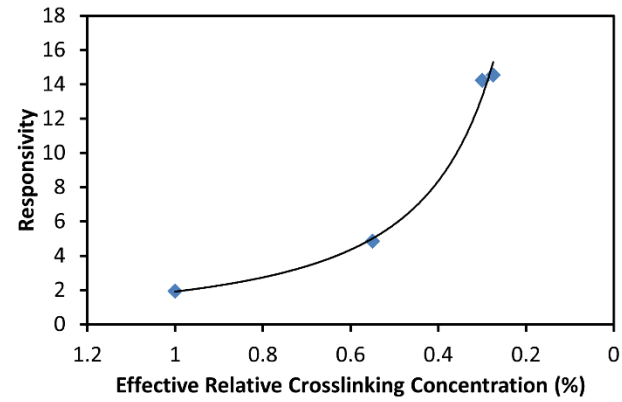


**Figure 4 Hydrogel responsivity dependence on Effective Relative Crosslinking Concentration (ERC). The data fit the relationship Responsivity≈2*ERC$^{-1.5}$.**